Integrative Bioinformatics Analysis Reveals miR-524-5p/MEF2C Regulates Bone Metastasis in Prostate Cancer and Breast Cancer

Qinghua Tian
Shanghai 6th Peoples Hospital Affiliated to Shanghai Jiaotong University
Yingying Lu
Shanghai 6th Peoples Hospital Affiliated to Shanghai Jiaotong University
Bicong Yan
Shanghai 6th Peoples Hospital Affiliated to Shanghai Jiaotong University
Chun-gen Wu (wucgsh@163.com)
Shanghai 6th Peoples Hospital Affiliated to Shanghai Jiaotong University

Research

Keywords: miR-524-5p, MEF2C, Bioinformatics Analysis, Bone Metastasis

Posted Date: November 9th, 2021

DOI: https://doi.org/10.21203/rs.3.rs-1029199/v1

Abstract

Background

Bone metastases are high prevalence in advanced prostate cancer and breast cancer patients, which have a serious impact on the quality of life and survival time of patients. Abnormal expression of microRNAs (miRNAs) has been reported in different types of cancer and metastasis. However, the underlying miRNAs associated with prostate and breast cancer bone metastasis remains unknown.

Methods

We performed bioinformatics analysis for TCGA cohort to identify differentially expressed miRNAs (DE-miRNAs) and their targets in the metastatic process.

Results

QPCR confirmed that miR-524-5p expression was down-regulated in prostate and breast cancer cell. And miR-524-5p over-expression restrained cell proliferation, invasion and metastasis ability in prostate and breast cancer. Meanwhile, miR-524-5p specifically targeting MEF2C was verified by luciferase assay.

Conclusions

In conclusion, our data strongly suggests down-regulation of miR-524-5p appears as a precocious event in prostate and breast cancer, and MEF2C emerges as a new player in prostate and breast cancer bone metastasis.

Background

Prostate cancer and breast cancer are the two most common invasive cancers in women and men, respectively. In terms of anatomy and physiological function, these cancers arise from different organs. However, both prostate and breast require gonadal steroids for their development, and tumors that arise from them are typically hormone-dependent and have remarkable underlying biological similarities[1]. As metastatic disease, the hormone therapy has become a standard of care in receptor-positive breast and prostate cancer. However, although hormone therapy has an effect on the inhibition of breast and prostate tumors initially, 70% of metastatic prostate and breast cancer patients harboring bone metastasis[2], showing a poor prognosis. In addition, prostate cancer and breast cancer is malignancy that are destined to become metastatic if screening has been unable to identify at an earlier stage before symptoms appear[3], causing serious threat to patients' life.

Bone is the most preferential metastatic site in prostate cancer[4] and breast cancer[5]. Once cancer has metastasized to the bones, it leads to numerous skeletal-related events (SREs) including intractable pain, fracture, bone marrow aplasia, spinal cord compression or nerve compression syndrome[6], which can rarely be cured and result in significant morbidity in patients of prostate cancer and breast cancer[7]. Despite its morbidity, the biology of bone metastasis is one of the most intriguing and complex of all oncogenic processes, which process can be separated into three key steps: seeding, dormancy, and outgrowth[8]. Therefore, all process in the metastatic process and the interaction with host cells can be served as valid therapeutic targets for the treatment of bone metastasis and tumor progression of prostate cancer and breast cancer.

MicroRNAs (miRNA or miR-) are single-stranded non-coding RNAs about 21-25 nucleotides long that are evolutionarily conserved and endogenously produced. MiRNAs play important gene-regulatory roles by targeting the 3'untranslated region (3'UTR) of mRNAs to mainly repress their expression[9]. Over the past several years, amounts of miRNA has been found and characterized in pathogenesis of many human malignancies, including various cancer metastasis and critical chemokines or cytokines in the bone microenvironment[10, 11]. For example, Wei-Luo et al found that miR-124 inhibits bone metastasis of breast cancer by repressing Interleukin-11[12]. MiR-133a-3p inhibits bone metastasis of prostate cancer[13]. In addition, evidence showed that abnormal expressions of miRNAs are highly associated with the occurrence and development of many cancer types, including, colon cancer[14], melanoma[15], gastric cancer[16], osteosarcoma[17], ameloblastoma in[18] and particular, breast cancer[19]. Once, Jin's studies have identified miR-524-5p as a tumor suppressor. Furthermore, miR-524-5p could inhibit migration, invasion, and epithelial-mesenchymal transition and progression in breast cancer cells[19]. However, little is known about its function on bone metastases from prostate and breast cancer.

Here for the first time, we clarified the role of cancer cell-derived miR-524-5p in bone metastases from prostate cancer and breast cancer and identified that perturbation of the miR-524-5p/MEF2C regulatory axis contributes to the bone metastasis observed in prostate cancer and breast cancer. These findings might provide novel therapeutic and diagnostic targets for bone metastases from breast cancer and prostate cancer.

Methods

mRNA and miRNA expression profiles download

We compared genes and miRNAs expression between patients with primary prostate and breast cancer with bone metastatic prostate and breast cancer. The gene expression profiles and the miRNA expression profile were obtained from Gene Expression Omnibus (GEO) database (https://www.ncbi.nlm.nih.gov/geo/). One dataset, with GEO accession number GSE32269, was deposited by Cai C et al[20], which contains 22 primary prostate cancer (hormone-dependent) versus 29 metastatic prostate cancer. Another dataset named GSE137842 was submitted by Lefley D[21] which contains 3 primary breast cancer and 3 metastasized to bone breast cancer. The two datasets were

obtained from Affymetrix Human Genome U133 Plus 2.0 Array. The miRNA microarray dataset, GSE26964[22], was composed entirely of 6 primary prostate cancer samples and 7 bone metastatic prostate cancer samples (platform: Capitalbio mammal microRNA V3.0).

Identification of differentially expressed miRNAs and differentially expressed gene

Herein, the gene and miRNA expression profile data preprocessing included background correction, quantile normalization, and probe summarization[23]. Then, R software and limma package in Bioconductor were used to extract differentially expressed miRNAs (DE-miRNAs) and differentially expressed genes (DEGs)[24] following criterion P-value < 0.05, $|\log_2 \text{fold change}| > 1$.

GO and KEGG pathway annotation

The identified common DEGs and DE-miRNAs were further subject to Gene Ontology consortium (GO, http://www.geneontology.org/) and Kyoto Encyclopedia of Genes and Genomes (KEGG, http://www.genome.jp/kegg/) functional enrichment using online tool of DAVID (Database for Annotation, Visualization and Integrated Discovery)[25]. GO analysis was performed for the cellular component (CC), biological process (BP), and molecular function (MF) categories[26] and KEGG pathway enrichment analysis for the selected genes (hypomethylated genes with high expression and hypermethylated genes with low expression)[27]. All parameters were set as default, p value < 0.01 was considered statistically significant.

mRNA-miRNA regulation network construction

Four databases including miRDB, TargetScan, miRanda, miTarbase, mirwalk was used to identify the number of miRNA-regulated target gene pairs. The threshold of correlation coefficient was set as -0.3 and significance P value was set as 0.05. The pairs supported by two or more databases were further processed and retained. Regulatory network visualization for the regulatory relationship between miRNA-mRNA was conducted using Cytoscape[28].

PPI network and hub genes analysis

The Search Tool for the Retrieval of Interacting Genes (STRING) database was used to detect the interactions of the DEGs, with confidence scores >0.7 were considered significant. PPI network further was visualized by Cytoscape. The cytoHubba plug-in and Molecular Complex Detection (MCODE) plug-in were used to identify hub genes and screen modules of the PPI network. All of the parameters of plug-in were left as the defaults. The genes in modules and hub genes were also analyzed by Metascape.

Prognostic analysis of hub genes

The survival data were extracted from each sample that was acquired from the clinical information of the above samples downloading from the TCGA, and combined with the previously obtained expression

profiling data, which were applied to the K-M survival curve drawing for each node by using R survival40, and the prognostic differences of the hub gene-MEF2C genes were analyzed.

Cell culture

The human prostate cancer cell lines DU145, LNCAP and breast cancer cell line MCF7 were obtained from COWELDGEN SCIENTIFIC (Coweldgen scientific Co.,LTD, Shanghai, China). DU145 and MCF-7 cells were grown in Minimum Essential medium (MEM, Life Technologies, USA) supplemented with 10% fetal bovine serum (FBS, Life Technologies, USA). LNCAP were cultured in RPMI 1640 medium (Life Technologies, USA) containing 10% FBS. All medium used in the study were supplemented with penicillin (100 U/ml) and streptomycin(100 mg/ml) (Biosharp, China). All cell lines were grown under a humidified atmosphere of 5% CO2 at 37 °C.

Cell transfection

Cells were seeded on 6-well plate, transfection was performed until cell density reached 70-80% at room temperature. MiR-524-5p mimics and normal control (NC) were designed through the reference of miRbase Database (www.miRbase.org and) and synthesized in GenePharma (Shanghai, China). Cells were transfected with 50nM miR-524-5p mimics or negative control using Lipofectamine 3000 (Invitrogen, USA) according to the manufacturer's instructions.

RNA extraction and RT-PCR analyses

Total RNA was extracted from cell lines with Trizol reagent (Invitrogen, USA) according to the manufacturer's instructions. 2.0 μg total RNA was reverse transcribed in a final volume of 20 μL using the PrimeScriptTM RT reagent Kit (Takara, Japan) according to the manufacturer's protocol. 0.5 μL complementary DNA (cDNA) was amplified and quantified on the LightCycler® 96 system (Roche, Switzerland) using SYBR® Premix Ex Taq™ II (Tli RNaseH Plus)(Takara, Japan). miRcute Plus miRNA First-Strand cDNA Kit (TianGen Biotech, Beijing, China) and SYBR Green (TianGen Biotech, Beijing, China) were used to quantify mature miRNA levels. U6 or beta-actin was used as the internal controls. Relative fold expressions were calculated with the comparative threshold cycle (2-ΔΔCt) method. The primers used are provided in supplementary Table 1.

Western blot

Total protein was extracted using the cell lysate for determining protein expression. Protein sample was quantified by bicinchoninic acid (BCA), separated by SDS-PAGE gel electrophoresis, and blocked with 5% skim milk. Membranes were then incubated with the primary antibody (Proteintech Group, Inc., Wuhan, China) and the corresponding secondary antibody (Beyotime Biotechnology, Shanghai, China). Band exposure was developed by chemiluminescence.

Dual-luciferase reporter gene assay

The MEF2C 3' UTR sequence containing wild-type and mutant binding sites was cloned into the pmirGLO luciferase vector. After the MEF2C 3'UTR WT (or MUT) were co-transfected with miR-524-5p mimic or negative control by Lipofectamine 3000 respectively. After 72 h, the cells were lysed and centrifuged at 12,000 rpm for 5 min to perform Dual-Lumi Luciferase Assay (Beyotime Biotechnology, Shanghai, China). The luciferase activity of the cells was determined by EnVision Multifunctional Microplate Reader (PerkinElmer, Germany). pmirGLO vector transfected into cells served as internal control.

Cell Counting Kit-8 (CCK-8) assay

100 μL of cell suspension containing 1×104 cells was added in each well of the 96-well plate. At 6 hrs, 24 hrs, 48 hrs, 72 hrs, and 96 hrs, 10 μL of CCK-8 reagent (Beyotime Biotechnology, Shanghai, China) was supplied, respectively. After cell culture for 2 hrs, the absorbance value of each well at 450 nm wavelength was measured by a microplate reader for plotting a growth curve.

Transwell assay

Cell suspension with 1×10^5 cells/mL was prepared with serum-free medium. 100 μL of the suspension was supplied into the chamber and 600 μL of complete medium was added in the basolateral chamber. At the other day, un-penetrating cells above the chamber were wiped off. Subsequently, the chamber was fixed in 4% paraformaldehyde for 30 mins and dyed with 1% crystal violet for another 10~15 mins. Five randomly selected fields in each sample were captured using an inverted microscope (magnification 100×).

In intro 3D model of prostate and breast cancer metastasis

All mouse experiments were approved by The Institutional Animal Care and Use Committee of ShangHai Sixth People's Hospital. To simulate in vivo bone metastasis microenvironment, one-day-old neonatal CD-1 mice were used to build an in vitro 3D model. In details, after CD-1 mice were sacrificed, their calvaria bone were separated under sterile condition and cut in the occipital lobe to produce an arch structure[29]. Then the calvarial bones were washed with PBS (pH 7.4) and were co-cultured with DU145 cells or MCF7 cells and DU145 cells or MCF7 cells transfected with miR-524-5p mimic in the 48-well plate at a density of 5×10^5 cells per well. The cranium bones without culturing with cells was set as negative control. After incubated at 37 °C for 4 days, the crystal violet staining experiment was performed: the bone fragments were taken out, fixed with 95% alcohol for 10 minutes, washed with PBS 3 times, and stained with 5 mg/mL crystal violet for 15 minutes. Wash the stained bone slices with PBS 3 times and observe under an inverted microscope. Each bone slice is randomly taken from 3 different fields to count the adhered cells (magnification 400×)[30, 31].

Statistical processing

SPSS 22.0 software (SPSS Inc., Chicago, IL, US) was utilized for statistical analysis. The quantitative data were represented as mean ± SD ($\bar{x}\pm s$). The independent t-test was used for analyzing the

measurement data. Chi-square test was applied for analyzing the categorical data. $P<0.05$ was considered statistically significant.

Results

Identification of DE-miRNAs and DEGs

A total of 870 DEGs from prostate cancer gene expression profiles were obtained, of which 387 were up-regulated and 483 were down-regulated (Figure 1A, B). And a total of 1790 DEGs from breast cancer gene expression profiles were obtained, of which 899 were up-regulated and 891 were down-regulated (Figure 1C, D). A total of 77 DE-miRNAs were obtained from breast cancer miRNA expression profiles, of which 37 were upregulated and 40 were downregulated (Figure 1E, F). We overlapped the DEGs (mRNA) screened in the prostate cancer bone metastasis dataset and breast cancer bone metastasis, and identified 22 upregulated and 27 down-regulated DEGs (Figure 1G, H).

Pathway and process enrichment analysis of DEGs

For the selected common DEGs, pathway and process enrichment analysis were performed through GO processes and KEGG pathways. The top 15 clusters from 3 categories with their representative enriched terms were shown in Figure 2A. The terms enriched in the biological process (BP) category included the cardiac tissue and animal organ development, cardiac muscle cell differentiation, embryonic organ morphogenesis, bone development, bone morphogenesis. The molecular function category showed enrichment for factors involved in the extracellular exosome, collagen-containing extracellular matrix, cell-subtrate adherens junction, focal adheren. In addition, the GO cell component category revealed enrichment in the cadherin binding, ribonuclease activity, retinoid binding, DNA binding, enhancer binding, aminopeptidase activity.

The results of the KEGG pathway enrichment analysis implied that common DEGs were significantly enriched in transcriptional mis-regulation in cancer, parethyroid hormone synthesis secretion and action, regulating pluripotency of stem cells, MAPK signaling, Ras signaling pathways, EGFR tyrosine kinase inhibitor resistance, endocrine resistance, prostate cancer, viral protein interaction with cytokine and cytokine receptor, FoxO adhesion molecules, gastric cancer , proteoglycans in cancer, endocytosis (Figure 2B, C).

mRNA –miRNA regulation network and PPI network construction

We used four target prediction databases to identify the target genes of selected DE-miRNAs and DEGs. In total, 49 genes which had different expression between patients with primary prostate and breast cancer and patients with bone metastatic prostate and breast cancer, were identified for 77 DE-miRNAs. In addition, nineteen of the target genes (NAV3, MEF2C, GART, HOXB7, STC2, CADM3, RAPGEF5, MMP16, NCAM1, ZC3H7B, ASPN, CD163, MXRA5, RNASE6, ARID1A, CYP26A1, MAFB, DCN, MS4A6A) were up-regulated and twenty seven of which were down-regulated. The pairs supported by two or more

databases were further processed and retained. The miRNA–mRNA regulatory network includes: DE-miRNAs (n =31), and target genes (n = 46), as shown in Figure 3A. Among of those DEGs, MEF2C showed extremely high expressed in patients with bone metastatic prostate and breast cancer (Figure 3B), and MEF2C was one of the targets for miR-524-5p.

For the DEGs in bone metastasis, a PPI network were constructed through the string database from 20 proteins (confidence level of 0.4) consists of 34 nodes, 17 edges. The PPI network analysis showed that MEF2C, FGF2, NCAM1, TCF3 and MS4A6A were hub genes (Figure 3C).

Prognosis related molecules as potential markers

Kaplan-Meier analysis revealed that low expression of MEF2C was strongly and positively correlated with shorter survival compared to the control group, and low expression of MEF2C was strongly and positively correlated with longer survival compared to the control group (Figure 4A). Receiver operating curve (ROC) analyses were performed to evaluate the ability of MEF2C expression to discriminate between normal and tumor tissues. An area under the ROC curve (AUC) of 0.964 of 0.5 years, 0.523 of 2.5 years and 0.604 of 4.5 years was obtained suggesting that MEF2C expression can discriminate between malignant and non-malignant tissues and can be used as a diagnostic marker for prostate cancer. An area under the ROC curve (AUC) of 0.747 of 0.5 years, 0.6 of 2.5 years and 0.547 of 4.5 years was obtained suggesting that MEF2C expression can discriminate between malignant and non-malignant tissues and can be used as a diagnostic marker for breast cancer (Figure 4B). Univariate Cox regression analyses indicated that pathological M stage were related to overall survival ($P<0.001$). Univariate Cox regression analyses indicated that pathological disease stage, pathological TNM stage and lymph node were related to overall survival ($P<0.05$) (Figure 4C).

miR-524-5p over-expression restrained cell proliferation and invasion ability in prostate and breast cancer

We analyzed the DE-miRNAs and found miR-524-5p as one of most significantly down-regulated miRNAs in prostate and breast cancer with bone metastasis (Figure3A□B). To verify this result, we detected the miR-524-5p expression in the human prostate cancer cell lines DU145, LNCAP, and breast cancer cell line MCF7. RT-qPCR showed that miR-524-5p was lower in MCF7 and DU145 cell lines (Figure 5A).

To explore the biological role of miR-524-5p, we transfected miR-524-5p mimic into DU145 and MCF7 cell line. Transfection of miR-524-5p mimic significantly increased miR-524-5p expression in DU145 and MCF7 cells (Figure 5B). In the CCK-8 assay, miR-524-5p mimic repressed cell proliferation ability of DU145 and MCF7 (Figure 5C). In the transwell assay, miR-1224-5p mimic repressed DU145 and MCF7 cells invaded into the lower chamber (Figure 5D), indicating that the invasion ability of prostate and breast cancer is increased.

miR-524-5p specifically targets MEF2C

MEF2C, a member of the family of transcription factors, has been proposed as a new player in breast cancer brain metastasis development [32]. In contrast to miR-1224-5p, the MEF2C was upregulated in

prostate and breast cancer with bone metastasis, and MEF2C gene was predicted as a target for miR-631, miR-524-5p, miR-330-3p, miR-346 (Figure 3A). Thus, we transfected miR-524-5p mimic, qPCR result showed that MEF2C mRNA significantly decreased compared with control (Figure 6A), and Western blot demonstrated that MEF2C protein dramatically decreased while transfecting miR-524-5p mimic (Figure 6B). These data indicated that MEF2C is most likely the target of miR-524-5p.

TargetsScan predicted that the MEF2C 3'UTR sequence at 130-136 base (site-1) and 904-910 base (site-2) is possible targeted for miR-524-5p (Figure 6C). To further confirm the position that miR-1224-5p targeted MEF2C, we conducted luciferase reporter assays. For site-1, luciferase activities decreased in the cells cotransfected with wild-type MEF2C and miR-524-5p mimic compared with NC group. However, after co-transfection with MEF2C mutation (mut) and miR-524-5p mimic, no differences in the luciferase activities compared with their control group. For site-2, while cells co-transfected with wild-type MEF2C and miR-524-5p mimic, there is less change in the luciferase activities compared with their control group (Figure 6D). Therefore, MEF2C is mainly targeted by miR-524-5p at 130-136 site.

Effect of miR-524-5p on in vitro 3D model of prostate or breast cancer bone metastasis

In the control group not cultured with tumor cells, the calvaria bone tissue was smooth and flat. In the model group cultured with DU145 or MCF7 cells, many DU145 or MCF7 cells grow on the surface of calvaria bones. We measured the number of DU145 or MCF7 cells on the calvaria bone through crystal violet staining. There is a small amount of residual bone cells on the surface. However, there are a large number of tumor cells on the surface of the calvaria bones in the model group cultured with DU145 or MCF7 cells, and less in the model group cultured with DU145 or MCF7 cells co-transfected with miR-524-5p mimic(Figure 7A,7B), which proves that the normal calvaria bones has strong adhesion to tumor cells, the adhered tumor cells cause damage to the calvaria bone in the co-culture group. However, miR-524-5p over-expression repressed adhesion and metastasis to bone tissue.

Discussion

As we described previously, bone is the most common metastasis site for prostate and breast cancer. Prostate and breast cancer bone metastasis is a multistep process including tumor cells dissemination into circulation, homing to bone, and proliferation in bone tissue. A complicated network of molecular events play a crucial role in the development of metastasis to bone. However, the underlying mechanism was not fully understood. In this study, we identified a microarray gene expression profile and established a comprehensive genetic interaction network to reveal the critical role of several miRNAs, and particularly miR-524-5p, and their common target MEF2C upregulated in the bone metastasis development. These findings provide new insights for considering the altered miRNAs as potential biomarkers and MEF2C as a possible target for preventing or breaking prostate and breast cancer metastasis.

Several lines of literature reported that miRNAs play a key role in cancer progression and metastatic. We found that 40 miRNA was downregulated such as miR-63, miR-524-5p, miR-330-3p, miR-346 and 37 miRNA was upregulated such as miR-564, miR-602, miR-129-5p when searching for miRNAs with an

aberrant expression in prostate and breast cancer metastasis. Over-expressed miRNAs in various tumors have been found in cancer models to function as oncogenic miRNAs[33–36]. Other decreased expression miRNAs are suspected as tumor suppressors[37–39]. Among those miRNAs as revealed by bioinformatical target prediction, miR-524-5p emerged as the most promising and reported to be involved in various cancer through different mechanism. MiR-204-5p has been predicted as a tumor suppressor molecule in multiple types of cancers. Several studies have reported that the miR-204-5p was down-regulated in many kinds of tumors and acted as a potent tumor suppressor inhibiting tumor proliferation and metastasis, including glioma[40], colon cancer cells[41], papillary thyroid carcinoma[42], gastric cancer[16]. In breast cancer, Jin et al have found that miR-524-5p inhibited the progression of migration, invasion and epithelial-mesenchymal transition in breast cancer cells through targeting FSTL1[19]. Wen et al found that miR-204-5p inhibited breast cancer cells reproduction and enhanced cell apoptosis[43]. However, Yang et al recently reported that miR-194-5p increased cell proliferation, migration and invasion in different breast cancer cell lines by regulating Wnt/β-catenin signaling pathway[44]. Consistent with Yang's result, our study confirmed that miR-204-5p was downregulated and promoted cell proliferation and invasion ability in prostate or breast cancer. As for the reason of contradicting reports, on the one hand, heterogeneity of miR-204-5p may play an essential role according the cell line we use is the same as Yang et al. On the other hand, it may be a consequence that one single miRNA can regulate various genes and functions or influence the multiple factors expression in different cellular contexts[45].

Myocyte enhancer factor 2 (MEF2) protein family of transcription factors includes MEF2A, MEF2B, MEF2C, and MEF2D. It was reported that MEF2C widely expressed such as expressed in muscle, neuronal, chondroid, immune, and endothelial cells[46]. In addition, MEF2C have close connections with cancer cell uncontrolled proliferation and enhancement of invasion[47]. As far as cancer metastasis is concerned, a recent study reported that MEF2C was consistently expressed in breast cancer brain metastases and that its nuclear translocation was related to brain metastatic disease severity via VEGFR-2 and β-catenin signaling[48]. MEF2C was predicted to be regulated by miR-802-5p and miR-194-5p in breast cancer brain metastases. This indicates that MEF2C presents a role in tumor metastasis. Using miRDB, TargetScan, miRanda, miTarbase, MEF2C was identified as a target for miR-63, miR-524-5p, miR-330-3p, miR-346, and its expression was increased. We confirmed that MEF2C is specifically targeted by miR-524-5p and down-regulated in prostate and breast cancer cell. It was reported that MEF2C is involved in breast cancer brain metastases. However, whether miR-524-5p function its roles in prostate and breast cancer metastasis via MEF2C, and what the specific downstream mechanism is still needed to further investigation. Collectively, down-regulation of miR-524-5p appears as a precocious event in prostate and breast cancer, and MEF2C emerges as a new player in prostate and cancer bone metastasis development.

Declarations

Ethics approval and consent to participate

Not applicable.

Consent for publication

Not applicable.

Availability of Data and Materials

The datasets used and/or analyzed during the current study are available from the corresponding author upon reasonable request.

Competing interests

The authors declare that they have no conflicts of interest to report regarding the present study.

Funding

This work was sponsored by grant National Natural Science Foundation of China [grant number 81701798, 81703751], Natural Fund from Shanghai Science and Technology Commission [grant number 18ZR1429400, 19411971800], and Natural Fund from Shanghai Municipal Health Commission [grant number 202040340], China.

Authors' contributions

Chungen Wu conceived the idea; Qinghua Tian performed the experiments; Yingying Lu and Bicong Yan analyzed the data; Chungen Wu wrote the manuscript and Qinghua Tian revised the manuscript. All authors have read and approved the final version of the manuscript.

Acknowledgements

Not applicable.

References

1. Risbridger GP, Davis ID, Birrell SN, Tilley WD: **Breast and prostate cancer: more similar than different**. *Nature Reviews Cancer* 2010, **10**:205–212.
2. Hernandez RK, Wade SW, Reich A, Pirolli M, Liede A, Lyman GH: **Incidence of bone metastases in patients with solid tumors: analysis of oncology electronic medical records in the United States**. *BMC Cancer* 2018, **18**:44.
3. Welch HG, Gorski DH, Albertsen PC: **Trends in Metastatic Breast and Prostate Cancer–Lessons in Cancer Dynamics**. *N Engl J Med* 2015, **373**:1685–1687.
4. Langley RR, Fidler IJ: **The seed and soil hypothesis revisited–the role of tumor-stroma interactions in metastasis to different organs**. *Int J Cancer* 2011, **128**:2527–2535.
5. Liu C, Wang L, Zhuang J, Liu L, Zhou C, Feng F, Sun C: **Should de-escalation of bone-targeting agents be standard of care for patients with bone metastases from breast cancer? A systematic review and**

meta-analysis. *Annals of Oncology* 2018, **29**:1329–1330.

6. Saad F, Lipton A, Cook R, Chen YM, Smith M, Coleman R: **Pathologic fractures correlate with reduced survival in patients with malignant bone disease**. *Cancer* 2007, **110**:1860–1867.
7. Tanaka R, Yonemori K, Hirakawa A, Kinoshita F, Takahashi N, Hashimoto J, Kodaira M, Yamamoto H, Yunokawa M, Shimizu C, et al: **Risk Factors for Developing Skeletal-Related Events in Breast Cancer Patients With Bone Metastases Undergoing Treatment With Bone-Modifying Agents**. *Oncologist* 2016, **21**:508–513.
8. Esposito M, Guise T, Kang Y: **The Biology of Bone Metastasis**. *Cold Spring Harb Perspect Med* 2018, **8**.
9. Wahid F, Shehzad A, Khan T, Kim YY: **MicroRNAs: synthesis, mechanism, function, and recent clinical trials**. *Biochim Biophys Acta* 2010, **1803**:1231–1243.
10. Lee YS, Dutta A: **MicroRNAs in cancer**. *Annu Rev Pathol* 2009, **4**:199–227.
11. Hesse E, Taipaleenmäki H: **MicroRNAs in Bone Metastasis**. *Curr Osteoporos Rep* 2019, **17**:122–128.
12. Cai WL, Huang WD, Li B, Chen TR, Li ZX, Zhao CL, Li HY, Wu YM, Yan WJ, Xiao JR: **microRNA-124 inhibits bone metastasis of breast cancer by repressing Interleukin-11**. *Mol Cancer* 2018, **17**:9.
13. Tang Y, Pan J, Huang S, Peng X, Zou X, Luo Y, Ren D, Zhang X, Li R, He P, Wa Q: **Downregulation of miR-133a-3p promotes prostate cancer bone metastasis via activating PI3K/AKT signaling**. *J Exp Clin Cancer Res* 2018, **37**:160.
14. Zhou WY, Cai ZR, Liu J, Wang DS, Ju HQ, Xu RH: **Circular RNA: metabolism, functions and interactions with proteins**. *Mol Cancer* 2020, **19**:172.
15. Nguyen MT, Lin CH, Liu SM, Miyashita A, Ihn H, Lin H, Ng CH, Tsai JC, Chen MH, Tsai MS, et al: **miR-524-5p reduces the progression of the BRAF inhibitor-resistant melanoma**. *Neoplasia* 2020, **22**:789–799.
16. Zhu CY, Meng FQ, Liu J: **MicroRNA-524-5p suppresses cell proliferation and promotes cell apoptosis in gastric cancer by regulating CASP3**. *Eur Rev Med Pharmacol Sci* 2019, **23**:7968–7977.
17. Yang H, Cao C, Wang LJ: **[LncRNA LINC-PINT regulating proliferation and apoptosis of osteosarcoma cells by targeting miR-524-5p]**. *Zhonghua Zhong Liu Za Zhi* 2020, **42**:325–330.
18. Chen L, Wang G, Qiao X, Wang X, Liu J, Niu X, Zhong M: **Downregulated miR-524-5p Participates in the Tumor Microenvironment of Ameloblastoma by Targeting the Interleukin-33 (IL-33)/Suppression of Tumorigenicity 2 (ST2) Axis**. *Med Sci Monit* 2020, **26**:e921863.
19. Jin T, Zhang Y, Zhang T: **MiR-524-5p Suppresses Migration, Invasion, and EMT Progression in Breast Cancer Cells Through Targeting FSTL1**. *Cancer Biother Radiopharm* 2020, **35**:789–801.
20. Cai C, Wang H, He HH, Chen S, He L, Ma F, Mucci L, Wang Q, Fiore C, Sowalsky AG, et al: **ERG induces androgen receptor-mediated regulation of SOX9 in prostate cancer**. *J Clin Invest* 2013, **123**:1109–1122.
21. Lefley D, Howard F, Arshad F, Bradbury S, Brown H, Tulotta C, Eyre R, Alferez D, Wilkinson JM, Holen I, et al: **Development of clinically relevant in vivo metastasis models using human bone discs and**

breast cancer patient-derived xenografts. *Breast Cancer Research* 2019, **21**.

22. Peng XS, Guo W, Liu TJ, Wang X, Tu XA, Xiong DF, Chen S, Lai YR, Du H, Chen GF, et al: **Identification of miRs-143 and-145 that Is Associated with Bone Metastasis of Prostate Cancer and Involved in the Regulation of EMT**. *Plos One* 2011, **6**.
23. Irizarry RA, Hobbs B, Collin F, Beazer-Barclay YD, Antonellis KJ, Scherf U, Speed TP: **Exploration, normalization, and summaries of high density oligonucleotide array probe level data**. *Biostatistics* 2003, **4**:249–264.
24. Ritchie ME, Phipson B, Wu D, Hu Y, Law CW, Shi W, Smyth GK: **limma powers differential expression analyses for RNA-sequencing and microarray studies**. *Nucleic Acids Res* 2015, **43**:e47.
25. Dennis G, Jr., Sherman BT, Hosack DA, Yang J, Gao W, Lane HC, Lempicki RA: **DAVID: Database for Annotation, Visualization, and Integrated Discovery**. *Genome Biol* 2003, **4**:P3.
26. Gene Ontology C: **The Gene Ontology (GO) project in 2006**. *Nucleic Acids Res* 2006, **34**:D322-326.
27. Ogata H, Goto S, Sato K, Fujibuchi W, Bono H, Kanehisa M: **KEGG: Kyoto Encyclopedia of Genes and Genomes**. *Nucleic Acids Res* 1999, **27**:29–34.
28. Shannon P, Markiel A, Ozier O, Baliga NS, Wang JT, Ramage D, Amin N, Schwikowski B, Ideker T: **Cytoscape: a software environment for integrated models of biomolecular interaction networks**. *Genome Res* 2003, **13**:2498–2504.
29. Curtin P, Youm H, Salih E: **Three-dimensional cancer-bone metastasis model using ex-vivo co-cultures of live calvarial bones and cancer cells**. *Biomaterials* 2012, **33**:1065–1078.
30. Alfred R, Taiani JT, Krawetz RJ, Yamashita A, Rancourt DE, Kallos MS: **Large-scale production of murine embryonic stem cell-derived osteoblasts and chondrocytes on microcarriers in serum-free media**. *Biomaterials* 2011, **32**:6006–6016.
31. Zhao YP, Ye WL, Liu DZ, Cui H, Cheng Y, Liu M, Zhang BL, Mei QB, Zhou SY: **Redox and pH dual sensitive bone targeting nanoparticles to treat breast cancer bone metastases and inhibit bone resorption**. *Nanoscale* 2017, **9**:6264–6277.
32. Sereno M, Hasko J, Molnar K, Medina SJ, Reisz Z, Malho R, Videira M, Tiszlavicz L, Booth SA, Wilhelm I, et al: **Downregulation of circulating miR 802-5p and miR 194-5p and upregulation of brain MEF2C along breast cancer brain metastasization**. *Molecular Oncology* 2020, **14**:520–538.
33. He L, Thomson JM, Hemann MT, Hernando-Monge E, Mu D, Goodson S, Powers S, Cordon-Cardo C, Lowe SW, Hannon GJ, Hammond SM: **A microRNA polycistron as a potential human oncogene**. *Nature* 2005, **435**:828–833.
34. Costinean S, Zanesi N, Pekarsky Y, Tili E, Volinia S, Heerema N, Croce CM: **Pre-B cell proliferation and lymphoblastic leukemia/high-grade lymphoma in E(mu)-miR155 transgenic mice**. *Proc Natl Acad Sci U S A* 2006, **103**:7024–7029.
35. Esquela-Kerscher A, Slack FJ: **Oncomirs - microRNAs with a role in cancer**. *Nature Reviews Cancer* 2006, **6**:259–269.

36. Voorhoeve PM, le Sage C, Schrier M, Gillis AJM, Stoop H, Nagel R, Liu YP, van Duijse J, Drost J, Griekspoor A, et al: **A genetic screen implicates miRNA-372 and miRNA-373 as oncogenes in testicular germ cell tumors**. *Cell* 2006, **124**:1169–1181.
37. Calin GA, Dumitru CD, Shimizu M, Bichi R, Zupo S, Noch E, Aldler H, Rattan S, Keating M, Rai K, et al: **Frequent deletions and down-regulation of micro-RNA genes miR15 and miR16 at 13q14 in chronic lymphocytic leukemia**. *Proceedings of the National Academy of Sciences of the United States of America* 2002, **99**:15524-15529.
38. Yanaihara N, Caplen N, Bowman E, Seike M, Kumamoto K, Yi M, Stephens RM, Okamoto A, Yokota J, Tanaka T, et al: **Unique microRNA molecular profiles in lung cancer diagnosis and prognosis**. *Cancer Cell* 2006, **9**:189–198.
39. Welch C, Chen Y, Stallings RL: **MicroRNA-34a functions as a potential tumor suppressor by inducing apoptosis in neuroblastoma cells**. *Oncogene* 2007, **26**:5017–5022.
40. Chen LC, Zhang W, Yan W, Han L, Zhang KL, Shi ZD, Zhang JX, Wang YZ, Li YL, Yu SZ, et al: **The Putative Tumor Suppressor miR-524-5p Directly Targets Jagged-1 and Hes-1 in Glioma**. *Carcinogenesis* 2012, **33**:2276–2282.
41. Li X, Li ZT, Zhu Y, Li Z, Yao LH, Zhang LM, Yuan L, Shang Y, Liu JT, Li CJ: **miR-524-5p inhibits angiogenesis through targeting WNK1 in colon cancer cells**. *American Journal of Physiology-Gastrointestinal and Liver Physiology* 2020, **318**:G827-G839.
42. Liu H, Chen X, Lin T, Chen X, Yan J, Jiang S: **MicroRNA-524-5p suppresses the progression of papillary thyroid carcinoma cells via targeting on FOXE1 and ITGA3 in cell autophagy and cycling pathways**. *J Cell Physiol* 2019, **234**:18382–18391.
43. Liang WH, Li N, Yuan ZQ, Qian XL, Wang ZH: **DSCAM-AS1 promotes tumor growth of breast cancer by reducing miR-204-5p and up-regulating RRM2**. *Mol Carcinog* 2019, **58**:461–473.
44. Yang F, Xiao Z, Zhang S: **Knockdown of miR-194-5p inhibits cell proliferation, migration and invasion in breast cancer by regulating the Wnt/beta-catenin signaling pathway**. *Int J Mol Med* 2018, **42**:3355–3363.
45. Dykxhoorn DM: **MicroRNAs and metastasis: little RNAs go a long way**. *Cancer Res* 2010, **70**:6401–6406.
46. Dong C, Yang XZ, Zhang CY, Liu YY, Zhou RB, Cheng QD, Yan EK, Yin DC: **Myocyte enhancer factor 2C and its directly-interacting proteins: A review**. *Prog Biophys Mol Biol* 2017, **126**:22–30.
47. Ostrander JH, Daniel AR, Lofgren K, Kleer CG, Lange CA: **Breast tumor kinase (protein tyrosine kinase 6) regulates heregulin-induced activation of ERK5 and p38 MAP kinases in breast cancer cells**. *Cancer Res* 2007, **67**:4199–4209.
48. Takashima S, Usui S, Inoue O, Goten C, Yamaguchi K, Takeda Y, Cui S, Sakai Y, Hayashi K, Sakata K, et al: **Myocyte-specific enhancer factor 2c triggers transdifferentiation of adipose tissue-derived stromal cells into spontaneously beating cardiomyocyte-like cells**. *Sci Rep* 2021, **11**:1520.

Supplementary Tables

Supplementary Table 1 is not available with this version.

Figures

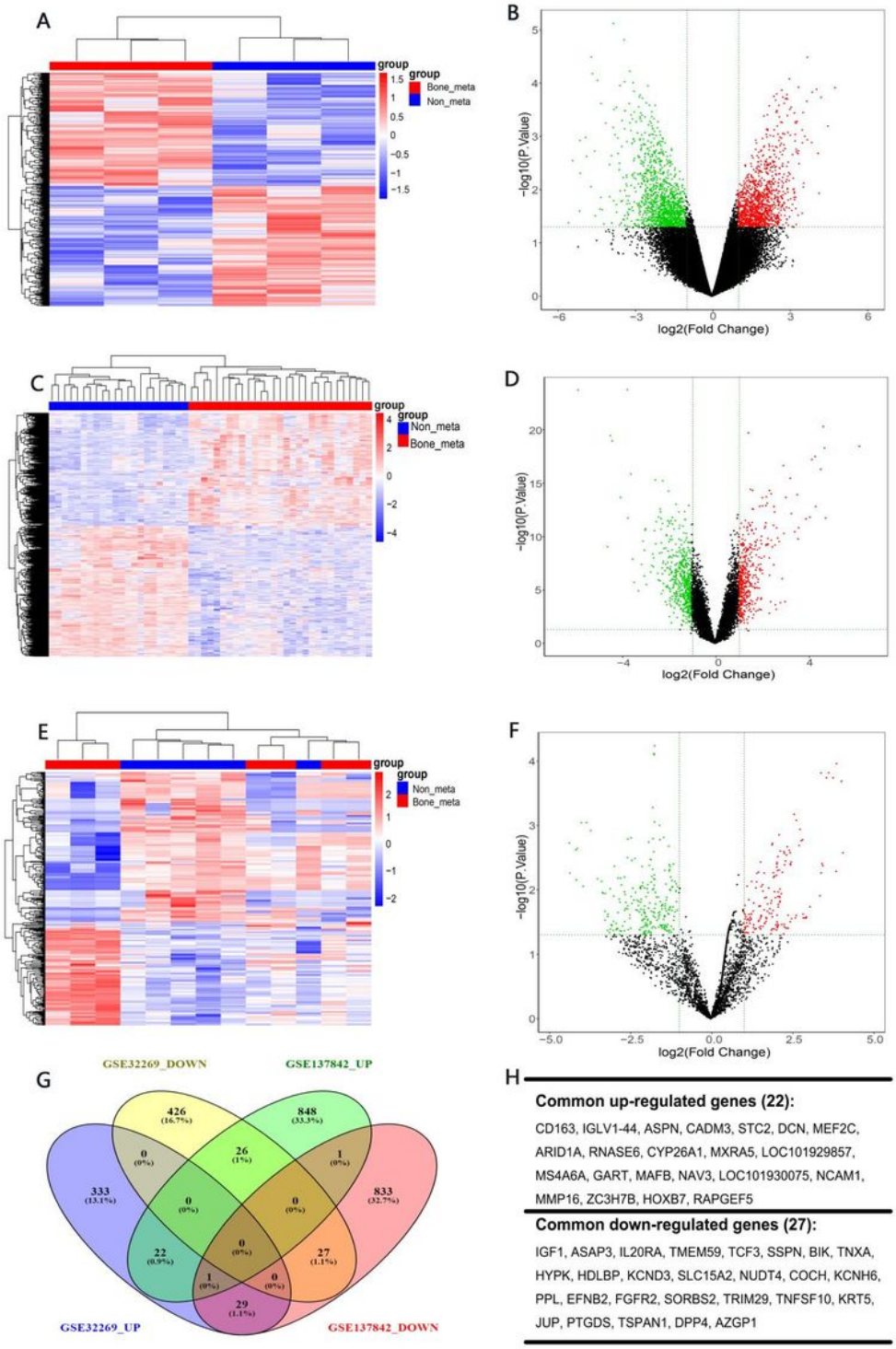

Figure 1

Identification of DE-miRNAs and DEGs related cancer bone metastasis A. Clustered heat map of the top 50 DEGs in GSE32269. Red: upregulated genes and blue: downregulated genes. B. Differentially expressed volcano plots in GSE32269. Green dots: significantly downregulated, red dots: significantly upregulated and black dots: no significant differences. C. Clustered heat map of the top 50 DEGs in GSE29079. Red: upregulated genes; blue: downregulated genes. D. Differentially expressed volcano plots in GSE29079. Green dots: significantly downregulated, red dots: significantly upregulated and black dots: no significant differences. E. Clustered heat map of the top 50 DE-miRNAs in GSE26964. Red: upregulated genes; blue: downregulated genes. F. Differentially expressed volcano plots in GSE26964. Green dots: significantly downregulated, red dots: significantly upregulated and black dots: no significant differences. G. The common DEGs from GSE32269 and GSE29079 involving in the prostate cancer bone metastasis and breast cancer bone metastasis by Venny 2.1.0.

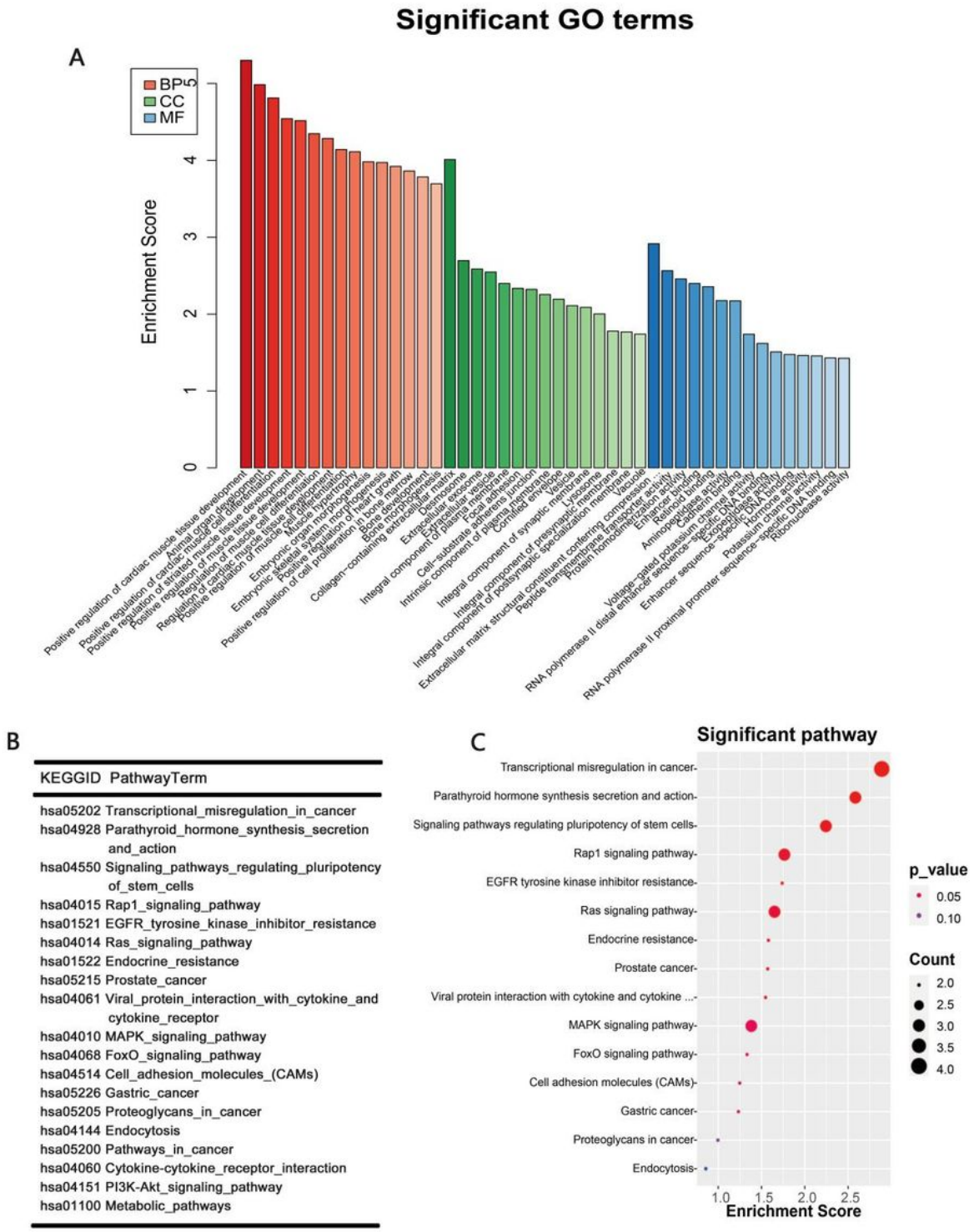

Figure 2

Visualizations of Pathway and process enrichment analysis results of DEGs. A. GO processes analysis of DEGs. The vertical axis represents the enrichment score value enriched on the GO term item, and the horizontal axis represents the name of the corresponding GO term item in the GO database. The figure only shows the top 15 of the three categories. BP: Biological Process MF: Molecular Function CC: Cellular Component. B. KEGG analysis of DEGs. The top 15 clusters with their representative KEGG pathways. The

color changes gradually from blue to red, which represents the significance level of enrichment to the pathway, and the redder in color, the more significant. The horizontal axis represents the enrichment score of the pathway, the vertical axis represents the corresponding pathway name in KEGG database, the size of the circle represents the number of genes enriched in the pathway. C. KEGG Pathway Enrichment Analysis of the DEGs.

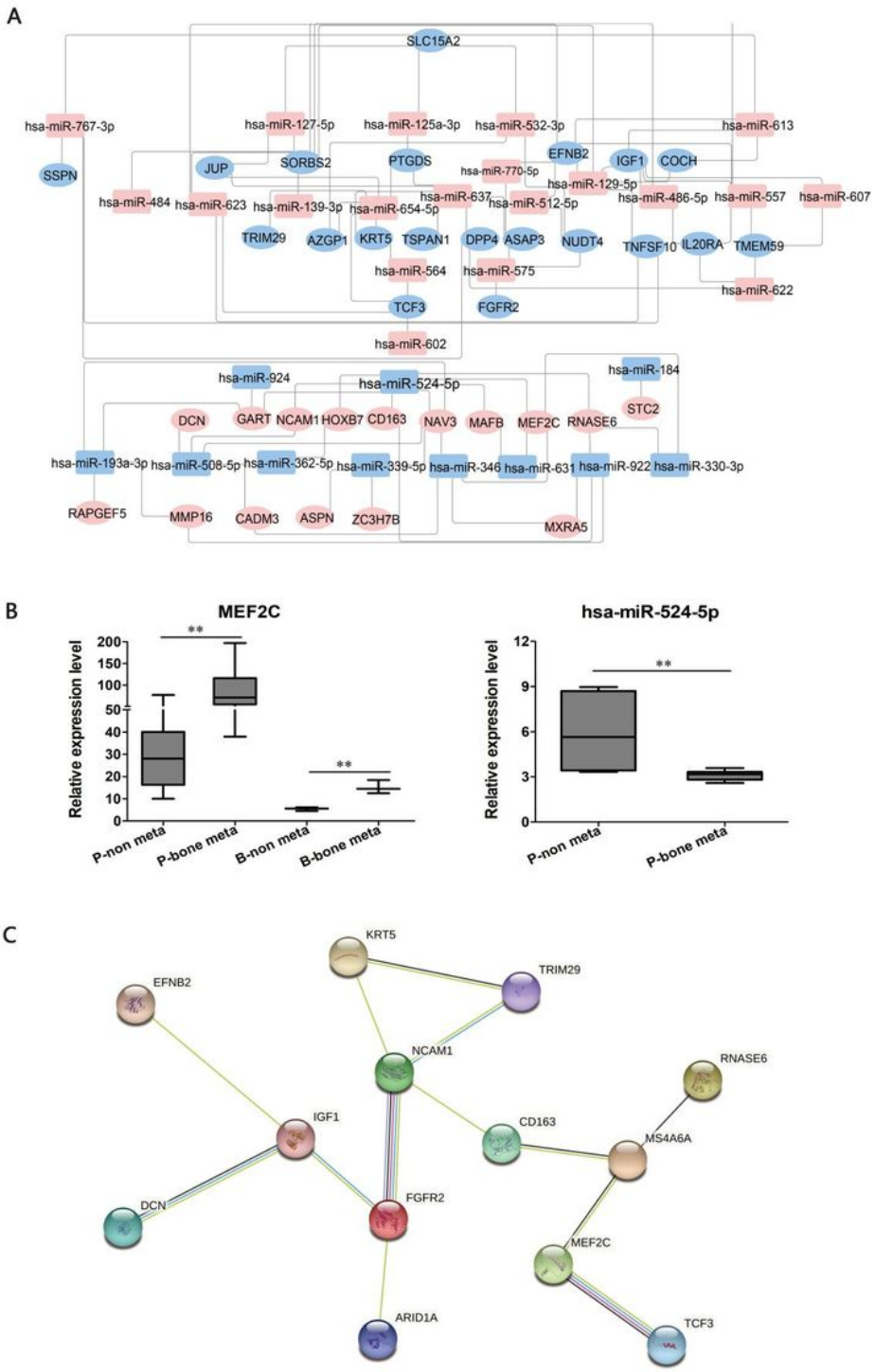

Figure 3

The landscape of mRNA-miRNA interaction and PPI networks. A. mRNA-miRNA interaction and PPI networks. Its graphic visualization uses different shapes representing different gene types, oval represents mRNA, square represents miRNA, and different colors represent different gene expression, red represents up-regulated genes, and blue represents down-regulated genes. B. Protein–protein interaction (PPI) network of the DEGs. The globules represent proteins, and the line between the globules represents the interaction between the two proteins.

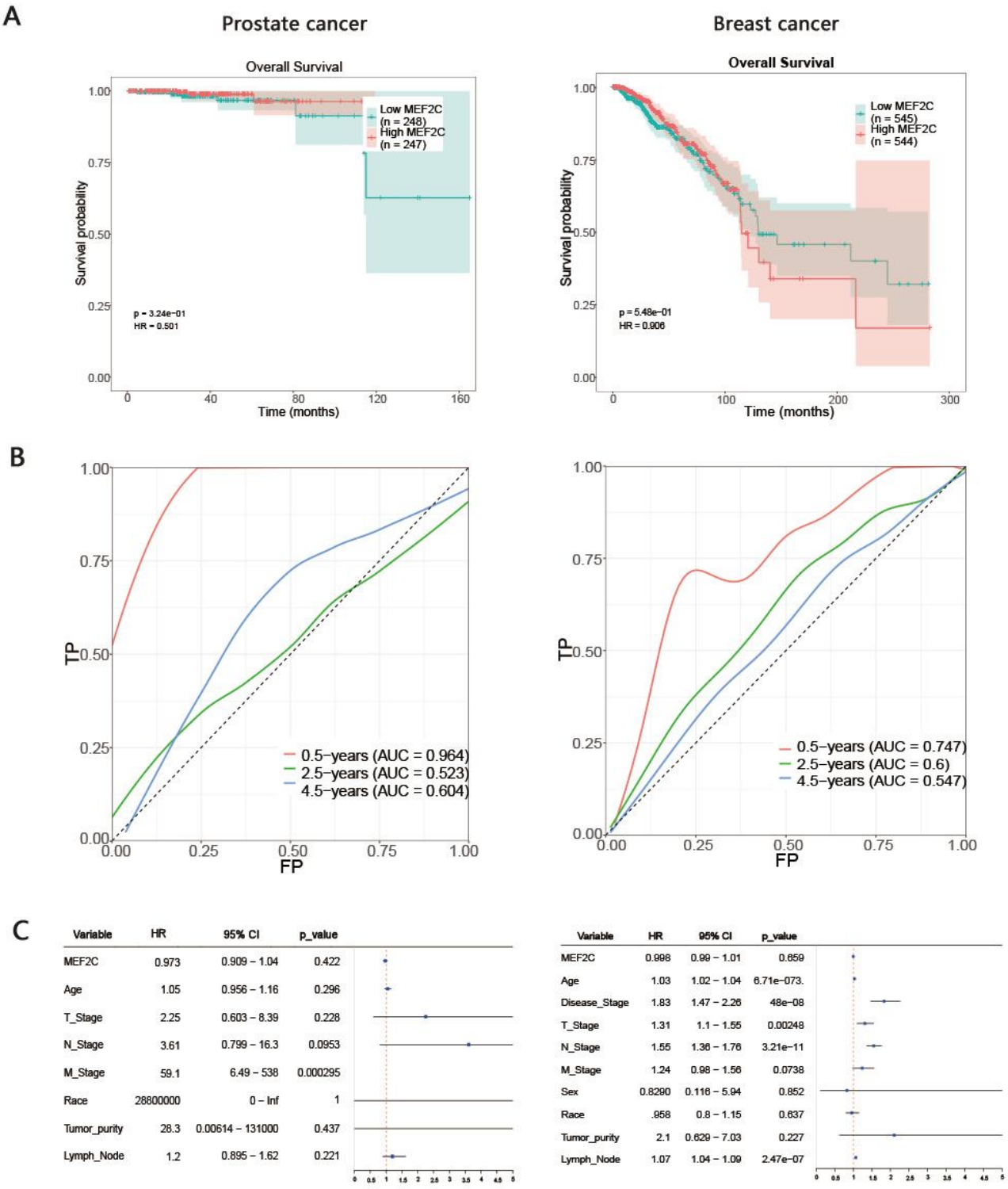

Figure 4

Prognosis Analysis of hub gene A. Kaplan-Meier analysis of overall survival curves of the prostate or breast cancer patients stratified by MEF2C expression. B. ROC curve analysis showing performance of MEF2C expression to discriminate in prostate or breast cancer patients. C. Univariate Cox regression analyses of overall survival.

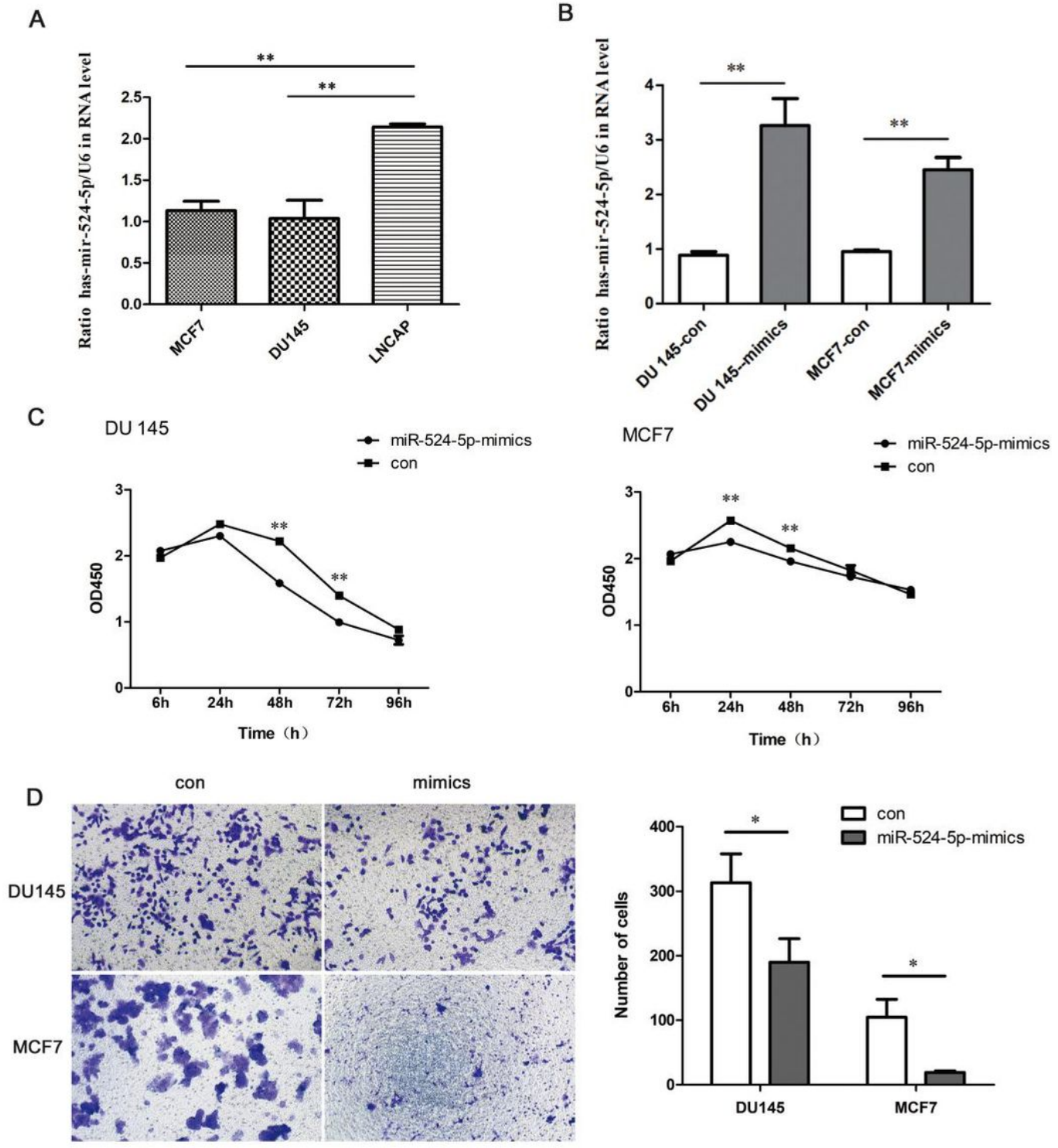

Figure 5

miR-524-5p repressed cell proliferation and invasion of DU145 or MCF7 cells. A. MiR-524-5p expression in RNA level was tested by qPCR method in MCF7, DU145, LNCAP cells. B. Transfection of miR-524-5p mimic increased miR-524-5p expression in DU145 or MCF7 cells. C. Overexpression of miR-1224-5p repressed proliferation of DU145 or MCF7 cells in a CCK-8 assay. D. Overexpression of miR-524-5p repressed cell invasion of DU145 or MCF7 cells in a Transwell assay.

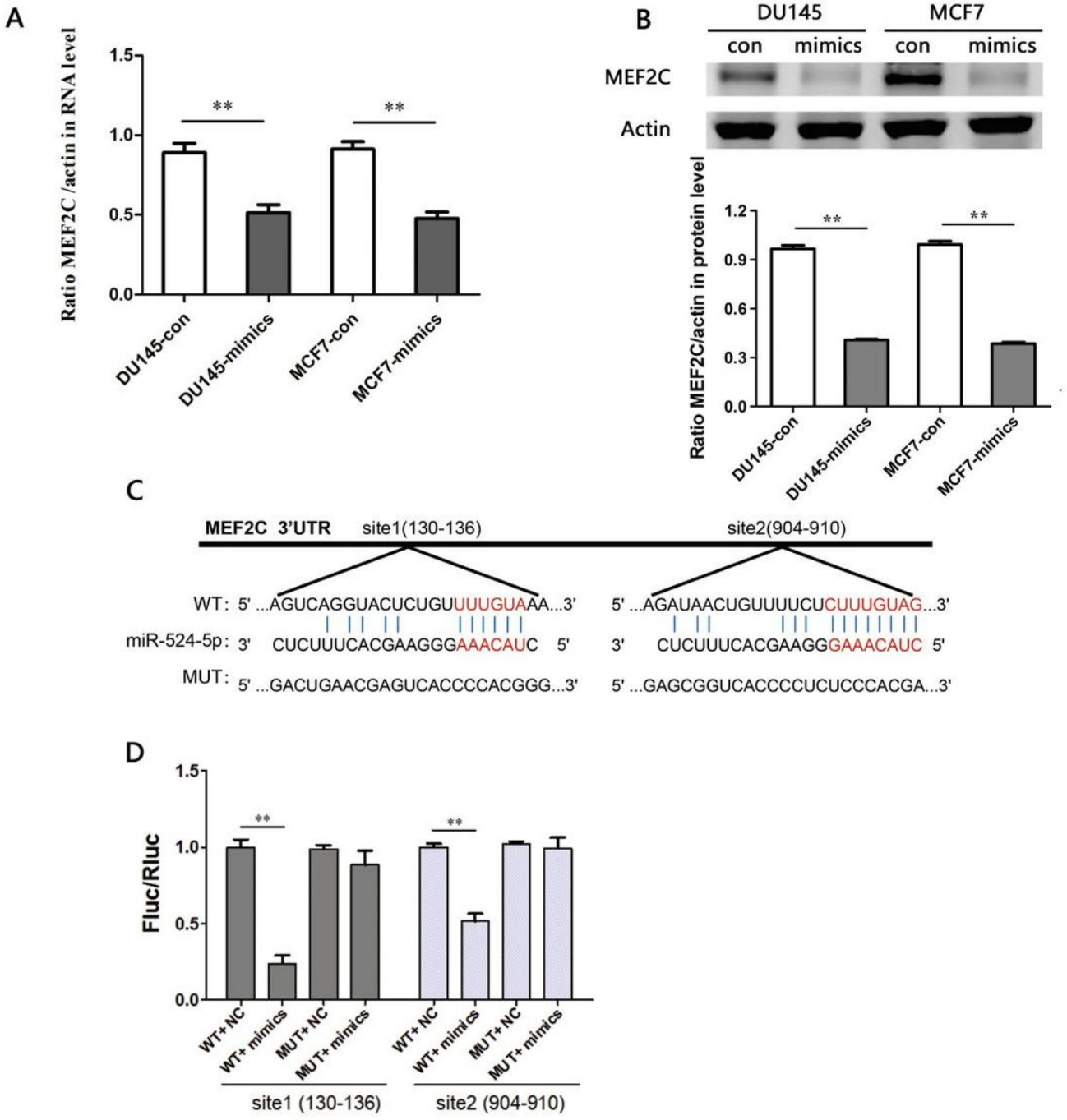

Figure 6

miR-524-5p specifically targets MEF2C A. qPCR resulted that the level of MEF2 was down-regulated after treatment with miR-524-5p mimic in DU145 and MCF-7 cells. B. Western blot analysis the expression of MEF2C protein in DU145 and MCF-7cells.C. Luciferase assay verified the relationship between miR-1224-5p and MEF2C.

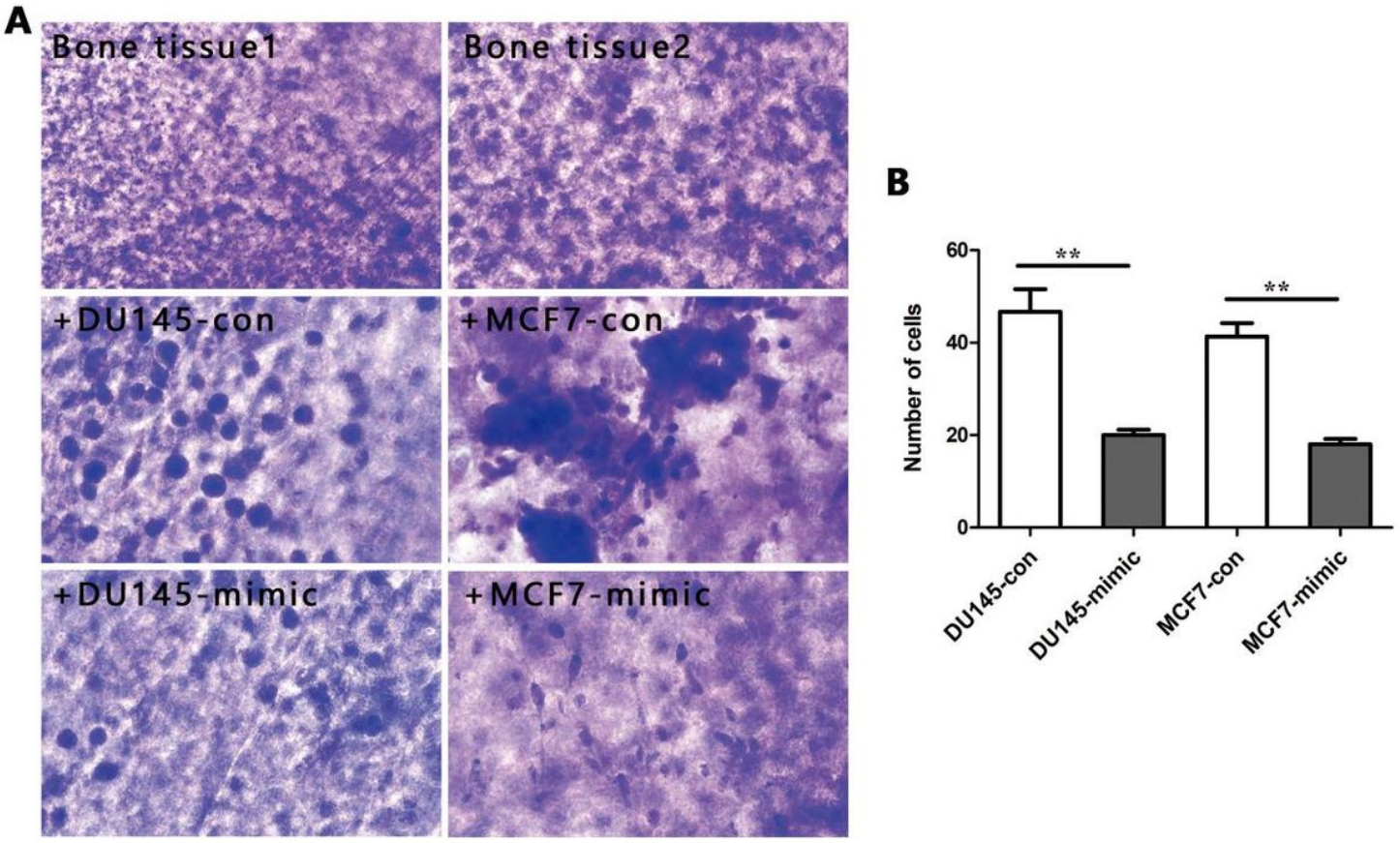

Figure 7

miR-524-5p promoted metastasis of DU145 or MCF7 cells in vitro 3D model A. Co-cultured bone tissue with MCF7 or DU145 cells with or without miR-524-5p mimic. B. Count and analyze the cells adhering to calvaria bone tissue